Lipid Solvation Effects Contribute to the Affinity of Gly-xxx-Gly Motif-Mediated Helix−Helix Interactions†

Rachel M. Johnson,‡,§ Arianna Rath,‡,§ Roman A. Melnyk,‡,§,|| and Charles M. Deber*,‡,§

Division of Structural Biology and Biochemistry, Research Institute, The Hospital for Sick Children, Toronto, Ontario, Canada M5G 1X8, and Department of Biochemistry, University of Toronto, Toronto, Ontario, Canada M5S 1A8

Received January 12, 2006; Revised Manuscript Received May 8, 2006

ABSTRACT: Interactions between transmembrane helices are mediated by the concave Gly-xxx-Gly motif surface. Whether Gly residues per se are sufficient for selection of this motif has not been established. Here, we used the in vivo TOXCAT assay to measure the relative affinities of all 18 combinations of Gly, Ala, and Ser "small-xxx-small" mutations in glycophorin A (GpA) and bacteriophage M13 major coat protein (MCP) homodimers. Affinity values were compared with the accessibility to a methylene-sized probe of the total surface area of each helix monomer as a measure of solvation by membrane components. A strong inverse correlation was found between nonpolar-group lipid accessibility and dimer affinity ($R = 0.75$ for GpA, $p = 0.013$, and $R = 0.81$ for MCP, $p = 0.004$), suggesting that lipid as a poor membrane protein solvent, conceptually analogous to water in soluble protein folding, can contribute to dimer stability and help to define helix−helix interfaces.

Although the forces that stabilize soluble protein folds have been extensively studied, the interactions that dictate the tertiary and quaternary structures of membrane proteins are incompletely understood (*1*). Because of the challenges presented by the hydrophobic nature of membrane proteins, only a handful of high-resolution structures have been elucidated (*2*−*7*). However, the folding of membrane proteins as described in the two-stage model (*8*−*10*) may be simpler than that of their soluble counterparts in that transmembrane (TM)[1] segments behave as individually stable, self-folding units that pack with one another to form the final protein structure. Adoption of tertiary (via intramolecular) and quaternary (via intermolecular) structures in the membrane thus depends upon TM helix−helix interactions, and the stability of these structures is a consequence of helix−helix affinities. One of the best-characterized motifs mediating TM helix−helix interactions, termed the Gly-xxx-Gly or GG4 motif, consists of two Gly residues separated by three variable intervening positions. The role of GG4 motifs in directing helix−helix interactions was initially implied in experimental and statistical searches (*11*−*13*). The $i-(i+4)$ distance between the Gly residues in this motif places both on the same α-helix face, producing a concave surface for close helix−helix contacts (*11*).

The precise role of Gly residues in this motif nevertheless remains an area of some debate. Some workers have found that Gly residues are sufficient but not necessary to determine helix−helix interactions (*14*), while others contend that Gly residues are neither necessary nor sufficient for the formation of dimers (*15*, *16*). We therefore chose to examine the importance of the concave helix surface created by the GG4 motif in determining interface selection and affinity by systematically replacing each Gly residue alone and in combination with Ala and Ser residues. These substitutions tend to fill in the Gly groove on the TM helix surface (Figure 1) and were therefore anticipated to reduce its ability to serve specifically as a nucleus of helix−helix assembly. Residue replacements were thus introduced into two well-characterized TM helices that form homodimers via GG4 motifs, the human erythrocyte protein glycophorin A (GpA) and bacteriophage M13 coat protein (MCP), because they have comparable folds (*17*). However, GpA is an obligate dimer optimized for high affinity, whereas the MCP dimer has moderate stability (*17*), a situation that allows the GG4 motif role to be evaluated in systems with variable helix−helix interaction strengths. In the present work, wild-type (WT) and mutant affinities were determined using the TOXCAT system, an in vivo assay that measures the extent of self-oligomerization in the *Escherichia coli* membrane (*18*).

EXPERIMENTAL PROCEDURES

Vectors and Strains. The expression vectors pccKAN, pccGpA-WT, and pccGpA-G83I, along with *E. coli* strain NT 326, were kindly provided by Dr. Donald M. Engelman, Yale University (*18*). Oligonucleotides encoding the TM

† This work was supported, in part, by a grant to C.M.D. from the Canadian Institutes of Health Research (CIHR). R.M.J. holds an Ontario Graduate Scholarship and a Research Training Committee award from the Hospital for Sick Children. A.R. holds a postdoctoral award from the CIHR Training Program in "Protein Folding: Principles and Diseases". R.A.M. held a CIHR doctoral award.

* To whom correspondence should be addressed: Telephone: (416) 813-5924. Fax: (416) 813-5005. E-mail: deber@sickkids.ca.

‡ The Hospital for Sick Children.

§ University of Toronto.

|| Present address: Department of Microbiology and Molecular Genetics, Harvard Medical School, Boston, MA 02115.

[1] Abbreviations: GpA, human erythrocyte protein glycophorin A; MCP, bacteriophage M13 coat protein; TM, transmembrane; GG4 motif, Gly-xxx-Gly motif; WT, wild type; MBP, maltose-binding protein; HRP, horseradish peroxidase; dpi, dots per inch; CAT, chloramphenicol acetyltransferase; ELISA, enzyme-linked immunosorbent assay; LASA, lipid-accessible surface area.

10.1021/bi060063f CCC: $33.50
Published on Web 06/27/2006

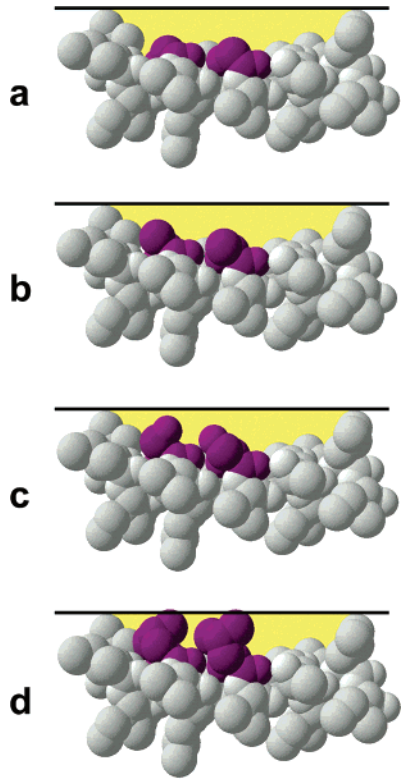

FIGURE 1: Infill of the concave GG4 motif surface by Ala and Ser substitutions. The van der Waals radii of residues 75−91 of the GpA TM helix are shown with the Gly residues at positions 79 and 83, colored purple. In comparison to (a) Gly, the (b) Ala and (c) Ser side chains reduce the depth of the concave surface (shaded in yellow) that serves to allow for the close approach of the two helices, while (d) Val residues interrupt the concave surface altogether. This figure was produced with Swiss PDB Viewer (*54*).

segment from MCP were restriction-digested with *Nhe*I and *Bam*HI and ligated into the *Nhe*I and *Bam*HI sites of the restriction-digested plasmid pccKAN. Individual mutants were produced by mutating either the WT GpA construct or the WT MCP construct using the QuikChange site-directed mutagenesis kit (Stratagene). Sequences of all constructs were confirmed using DNA sequencing and were subsequently transformed into *E. coli* NT 326 (*malE*$^-$) cells. To determine the expression level of each chimera, whole-cell lysates controlled for the number of cells were analyzed by Western blot using an antibody against maltose-binding protein (MBP) (NEB). Blots were developed with a goat anti-rabbit horseradish peroxidase (HRP) secondary antibody (Sigma), and band densitometry was performed using NIH image. Statistical analysis was performed using the software program R.

Chloramphenicol Acetyltransferase (CAT) Enzyme-Linked Immunosorbent Assay (ELISA). Constructs transformed into NT 326 cells were grown at 37 °C and 250 rpm to an A_{600} of 0.6. Cells were harvested into 1 mL fractions and stored at −80 °C. Cell lysates were prepared as previously described (*19*) and assayed for CAT concentration using the CAT ELISA kit (Roche Applied Science). A standard curve was generated with CAT provided by the manufacturer. In each experiment, the high-affinity GpA dimer, the lower affinity MCP dimer, and a mutant that disrupts dimerization of GpA (G83I) were included as controls. All measurements were performed in at least triplicate, and errors shown are standard deviations on at least three measurements. Statistical analysis was performed in the R software program.

MalE Complementation Test. M9 minimal medium plates were used with 0.4% maltose as the only carbon source (*18*). NT 326 cells transformed with each mutant were streaked onto the plates and incubated for 2 days at 37 °C.

Interfacial Residue Burial Calculations. The burial of TM segment residues in the GpA MCP dimer interfaces was estimated using NACCESS (*20*) as follows. Edited Protein Data Bank (PDB) files containing the TM regions of the GpA (*11*) (PDB ID 1AFO, residues 73−95) or MCP (*17*) (residues 27−45) dimers were submitted to NACCESS, and lipid-accessible surface area (LASA) of each residue in Å^2 was estimated using a probe of radius 1.88 Å. The 1.88 Å probe radius was selected to approximate the size of a methylene group on a lipid acyl chain and is the average of the methylene atomic radius calculated by two groups (*21*, *22*). Monomer accessibility was calculated using the above-mentioned structure files, where all atoms except those in a single monomer were deleted. The percent burial of each residue upon dimerization was determined using eq 1

$$(\text{residue LASA}_{\text{monomer}} - \text{residue LASA}_{\text{dimer}})/(\text{residue LASA}_{\text{monomer}}) \times 100 \quad (1)$$

Helix Solvation Calculations. The sequences of the WT and mutant GpA (residues 75−89) and MCP (residues 21−42) TM segments placed in the TOXCAT chimera (see Figure 2 for sequences) were modeled as single (monomeric) energy-minimized α-helices using the CNS program suite (*23*). The PDB files thus generated, each containing a single α-helix structure, were analyzed using NACCESS to estimate the LASA of each monomer as described above. Relative LASA values were obtained using a reference data set of LASA values calculated for each of the 20 amino acids when placed as the guest residue in a set of α-helical Gly-X-Gly tripeptides according to eq 2

$$\text{residue LASA}_{\text{relative}} = (\text{residue LASA}_{\text{helix}}/\text{residue LASA}_{\text{Gly-X-Gly}}) \times 100 \quad (2)$$

Per residue LASA values were determined by dividing the total helix LASA by the total number of helix residues. Total interfacial LASA values were determined as the sum of the individual LASA values of GpA residues Leu 75, Ile 76, Gly 79, Val 80, Gly 83, Val 84, and Thr 87 or MCP residues Val 30, Val 31, Gly 34, Ala 35, Gly 38, and Ile 39 (*17*). Statistical analysis was performed using the R software program.

RESULTS

Mutations in the GG4 Motif Have Different Effects on GpA versus MCP Affinity. A total of 18 TM helix sequences including WT GpA, WT MCP, and mutants representing all possible combinations of Gly, Ala, and Ser residues in their GG4 motifs (Figure 2) were incorporated into the TOXCAT vector pccKAN and expressed in the inner membrane of *E. coli* with an N-terminal fusion of the DNA-binding domain of ToxR and a C-terminal fusion of the periplasmic MBP (*18*). Homo-oligomerization of the TM domain in the TOXCAT system results in ToxR dimerization, thereby driving transcriptional activation of a CAT reporter gene.

a

GpA TM: ..LIIFGVMAGVIGTIL .. 75-89

MCP TM: ..YIGYAWAMVVVIVGATIGIKLF.. 21-42

b

GpA TM Series (75 - 87):

GG4	L	I	I	F	G	V	M	A	G	V	I	G	T
AG4	L	I	I	F	A	V	M	A	G	V	I	G	T
SG4	L	I	I	F	S	V	M	A	G	V	I	G	T
GA4	L	I	I	F	G	V	M	A	A	V	I	G	T
AA4	L	I	I	F	A	V	M	A	A	V	I	G	T
SA4	L	I	I	F	S	V	M	A	A	V	I	G	T
GS4	L	I	I	F	G	V	M	A	S	V	I	G	T
AS4	L	I	I	F	A	V	M	A	S	V	I	G	T
SS4	L	I	I	F	S	V	M	A	S	V	I	G	T

MCP TM Series (30 - 42):

GG4	V	V	I	V	G	A	T	I	G	I	K	L	F
AG4	V	V	I	V	A	A	T	I	G	I	K	L	F
SG4	V	V	I	V	S	A	T	I	G	I	K	L	F
GA4	V	V	I	V	G	A	T	I	A	I	K	L	F
AA4	V	V	I	V	A	A	T	I	A	I	K	L	F
SA4	V	V	I	V	S	A	T	I	A	I	K	L	F
GS4	V	V	I	V	G	A	T	I	S	I	K	L	F
AS4	V	V	I	V	A	A	T	I	S	I	K	L	F
SS4	V	V	I	V	S	A	T	I	S	I	K	L	F

FIGURE 2: Small substitution constructs for the GpA and MCP TM series. (a) GpA WT ($GG4_{GpA}$) and MCP WT ($GG4_{MCP}$) sequences. (b) GpA TM and MCP TM mutant sequences. Residues boxed in blue represent the two positions of the "Gly-xxx-Gly" motif; those boxed in gray are distal residues that modulate TM−TM helix affinity (*17*). Constructs are designated by a two-letter code that denotes the identity of the first and second "Gly-xxx-Gly" motif positions, i.e., AS4 = Ala-xxx-Ser with a subscript denoting the GpA or MCP TM background.

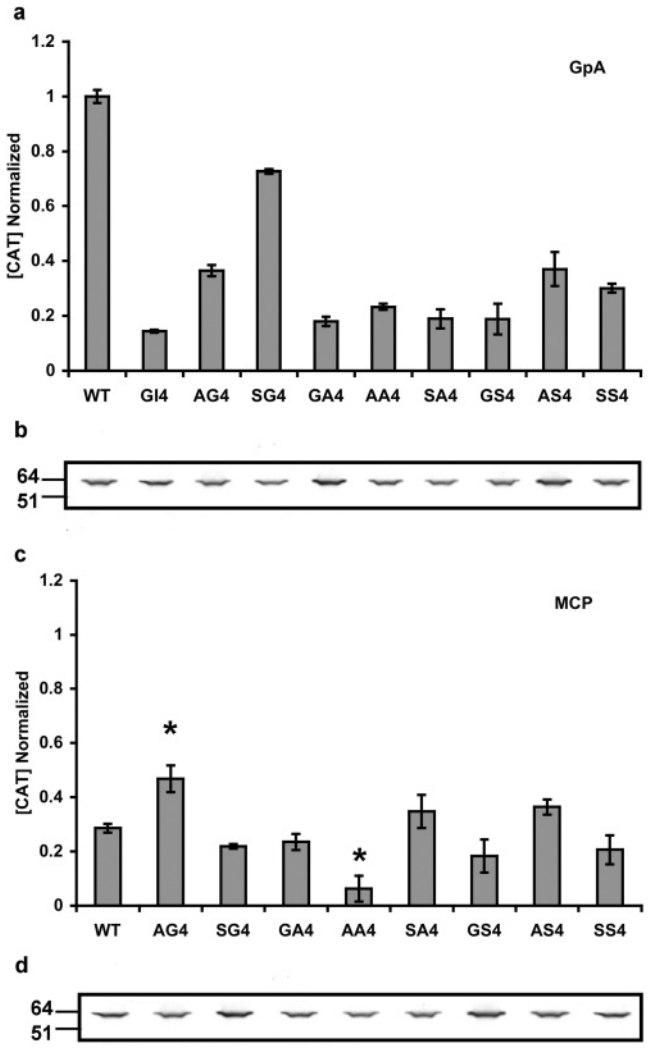

FIGURE 3: TOXCAT assay of WT and mutant GpA and MCP TM segments. CAT levels are normalized to WT GpA ($GG4_{GpA}$); the G83I GpA mutant ($GI4_{GpA}$) used as a negative control for dimerization is shown for comparison. (a) CAT levels of WT and mutant GpA constructs. (b) Expression levels of all GpA constructs. The lane order is the same as presented in a. (c) CAT levels of WT and mutant MCP constructs. (d) Expression levels of all MCP constructs. The lane order is the same as presented in c. Cell lysates of each construct were analyzed by Western blot using an α-MBP antibody. Error bars represent the standard deviation of at least three measurements for each construct. The asterisk indicates $p < 0.001$ (using the Tukey−Kramer multiple comparisons test) when compared with MCP WT ($GG4_{MCP}$).

Furthermore, the level of CAT expression correlates with the extent of TM helix-mediated association (*18*). A GpA mutant, G83I (denoted $GI4_{GpA}$), known to disrupt helix−helix association (*18*), was used as a negative control for dimerization.

The correct membrane insertion of each fusion protein was confirmed by the growth of NT326 cells expressing each fusion protein construct on M9-maltose plates (not shown). Western blotting, the accepted methodology used to normalize fusion protein expression in TOXCAT (*18*, *24*−*35*), in conjunction with densitometry measurements confirmed that each chimera was produced at comparable levels [the expression level of each construct compared to WT GpA for all experiments was identical with $p < 0.05$; average values were 166 ± 21 dots per inch (dpi) for GpA and 171 ± 19 dpi for MCP]. We therefore considered differences in the CAT amount measured in the ELISA assay to be the result of altered dimer affinity rather than changes in the expression level of the fusion protein (*vide infra*). WT GpA formed a greater proportion of the dimer than did WT MCP, evidenced by an increased CAT expression (Figure 3). WT MCP exhibited approximately 30% of the TOXCAT activity of WT GpA (Figure 3), compared to approximately 10% in a previous study (*17*). Such variation has been observed in TOXCAT signals: for example, the measured affinity of the GpA G83I mutant ranges from approximately 4% (*36*) to approximately 20% (*37*) of WT GpA values. Nevertheless, the hierarchy of stability of sequence variants tends to be conserved between these studies, and we find a linear correlation between the relative stability of our GpA variants versus the WT measured in the TOXCAT assay and the free energy of dimerization relative to the WT (*15*, *16*, *38*) (Figure 4). In our hands, the G83I substitution reduced the affinity of the GpA helix to approximately 14% of the WT value (Figure 3a).

Although replacements made individually at either Gly 79 or Gly 83 in GpA disrupted dimerization, Gly-83-substituted motifs formed lower affinity dimers than their Gly 79 counterparts (Figure 3). For example, the G83A and G83S replacements (denoted $GA4_{GpA}$ and $GS4_{GpA}$) decreased

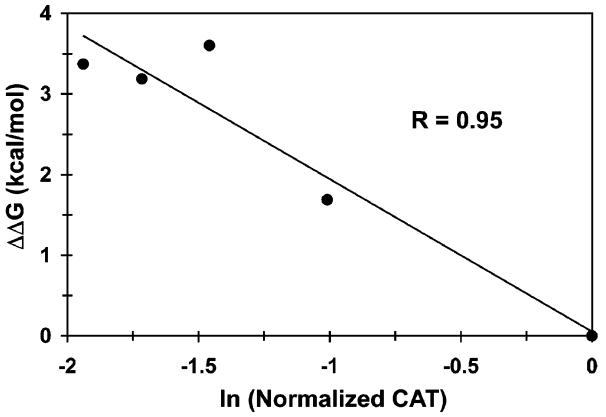

FIGURE 4: Comparison of normalized CAT production for WT (GG4) and mutant (AG4, GA4, GI4, and AA4) GpA constructs in the TOXCAT assay with their reported free energy of dimerization relative to WT GpA in detergent micelles (*15*, *16*).

affinity to levels equivalent to G83I ($GI4_{GpA}$, see Figure 3a), while substitution of Gly 79 in the Gly 83 background ($AG4_{GpA}$ and $SG4_{GpA}$) maintained helix affinity closer to WT levels. When both Gly positions were replaced, helix−helix association of the resulting mutants ($AS4_{GpA}$, $AA4_{GpA}$, $SA4_{GpA}$, and $SS4_{GpA}$) was also compromised (Figure 3a). The greater proportion of dimers formed by the $AS4_{GpA}$ versus $SA4_{GpA}$ mutant (Figure 3a) also indicates position 83 as less tolerant of residue substitutions than position 79. The dimerization ability of the $SS4_{GpA}$ mutant was greater than that of its $AA4_{GpA}$ counterpart, possibly because of the interactions promoted by the polarity of the Ser side chain. Within experimental error, the self-association of the $AG4_{GpA}$, $SG4_{GpA}$, $GA4_{GpA}$, and $GI4_{GpA}$ substitutions is comparable to homodimerization levels evaluated using the GALLEX assay (*14*). The $GS4_{GpA}$ mutant, however, exhibits approximately 20% of WT TOXCAT activity (Figure 3a) compared with about 80% of WT activity in the GALLEX system (*14*), a difference that may originate from the use of two distinct assay systems. Unlike GpA, small residue substitutions at Gly 34 and Gly 38 in MCP caused only minor variations in helix−helix affinity (Figure 3c), and each position was equivalent in terms of tolerating Ala and Ser replacements. Only two MCP mutants ($AG4_{MCP}$ and $AA4_{MCP}$) had significantly different dimerization values than WT ($GG4_{MCP}$); $AG4_{MCP}$ increased dimerization, while $AA4_{MCP}$ was disruptive (Figure 3c).

Small Residue Substitutions at the GG4 Motif Do Not Change the MCP Dimer Interface. We sought to determine if the changes in affinity of the GpA and MCP mutants were caused by disruption of the native helix−helix interfaces of each dimer or by other factors such as removal of van der Waals or electrostatic interactions across the native interface. As a test for interface preservation in the presence of "filled in" Gly residue grooves, substitutions known to confer high affinity to the MCP homodimer in the GG4 motif background (V30L and F42T) (*17*) were recreated in the MCP AS4 background. If the $AS4_{MCP}$ helix retains its WT dimerization site, these residue substitutions would be expected to similarly increase stability. Consistent with previous experiments (*17*), no significant change in dimer affinity occurred when the F42T substitution was introduced into the $AS4_{MCP}$ background (Figure 5). Similarly, the V30L and F42T double mutant (*17*) had a statistically significant increase in dimer-

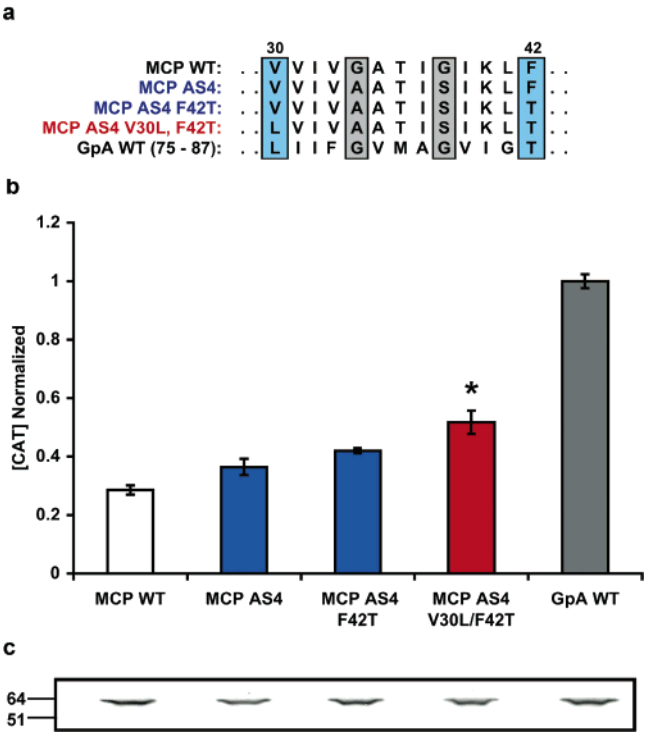

FIGURE 5: TOXCAT assay of distal residue mutants. (a) Sequence alignment of single- and double-mutant $AS4_{MCP}$ constructs are shown with WT MCP ($GG4_{MCP}$) and WT GpA ($GG4_{GpA}$). (b) Normalized CAT expression relative to WT GpA. Error bars represent the standard deviation of at least three measurements for each construct. The asterisk indicates $p < 0.01$ (using Tukey−Kramer multiple comparisons test) when compared with $AS4_{MCP}$. Colored bars correlate with the same colored sequences given in a. (c) Fusion protein expression levels of each construct assayed by TOXCAT. Cell lysates were analyzed by Western blot using an α-MBP antibody.

ization ($p < 0.01$). The degree of stabilization by the V30L and F42T double mutant observed in $AS4_{MCP}$ is likely less than the 3-fold increase in $GG4_{MCP}$ (*17*) because of the Ala and Ser replacement of the GG4 motif residues. On the basis of these results, we concluded that the GpA and MCP mutants are likely to retain their native oligomerization sites across this series of systematic motif replacements.

Close Packing of Interfacial Gly Residues Dictates Tolerance to Small Residue Substitution. Because the native helix−helix interface is largely preserved in the library of GG4 motif small residue mutants, we reasoned that affinity changes could be caused, in part, by a disruption of the stabilizing van der Waals and/or electrostatic interactions that depend upon close packing across the helix−helix interface. Residue burial in the native GpA and MCP interfaces was thus examined to see if changes in affinity could be rationalized by local packing differences at the two Gly positions in the GG4 motif. Using a methylene-sized probe to estimate the accessibility to membrane components of each residue in the GpA and MCP structures, we determined that Gly 79 and Gly 83 are indeed buried in the helix−helix interface of the WT GpA homodimer structure (*11*), as illustrated in Figure 6a. However, they are slightly nonequivalent in terms of close packing with neighboring residues, where Gly 79 averages 88% burial over each monomer and Gly 83 averages 92%. Gly 83 is therefore somewhat more tightly packed into the GpA interface than

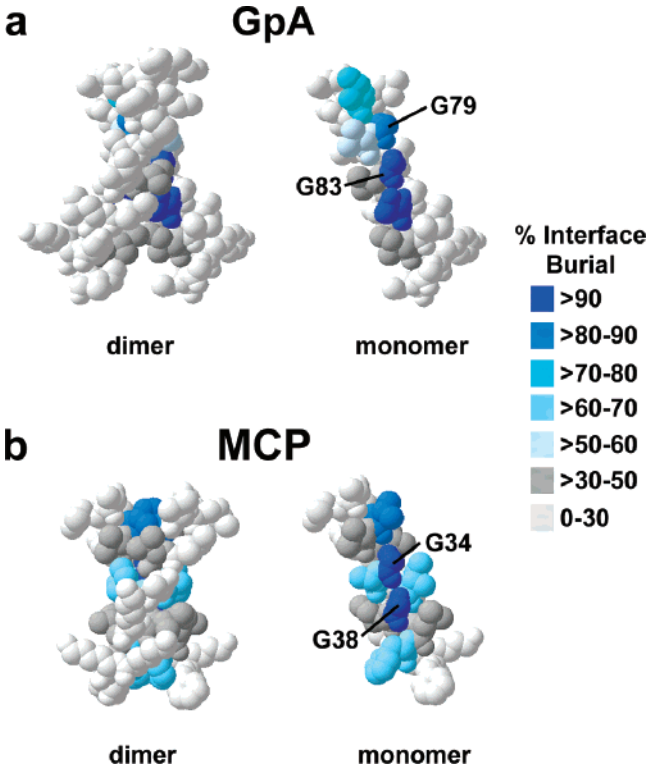

FIGURE 6: Residue burial in the GpA and MCP dimer interfaces. Space-filling models of the TM helix regions of (a) the GpA homodimer (*11*) (PDB ID 1AFO) and (b) the MCP model (*17*). Dimeric structures are shown on the left; on the right, the topmost helix has been removed to reveal the interfacial residues. Residues are shaded to show average percent burial in each dimer. This figure was produced with Swiss PDB Viewer (*54*).

Gly 79 and might be expected to be less tolerant to substitution, a finding that may explain, in part, the higher sensitivity of Gly 83 to residue replacement. A similar analysis of a structural model of the MCP homodimer (*17*) indicated that both Gly residues are 100% buried in the helix−helix interface (Figure 6b), providing an explanation for the essentially equivalent effects of Gly 34 and Gly 38 mutations in the latter case. However, we note that the structure analyzed is a model; a complete description of the effects of these substitutions may require high-resolution structure determination of MCP.

Accessibility of Monomer Surfaces to Lipid Inversely Correlates with Dimer Affinity. The above analysis of the GpA and MCP interfaces provided an explanation for the position specificity of the Gly residue replacements within a given GG4 motif. Dimers containing the GG4 motif can be further stabilized by $C_\alpha H-O$ hydrogen bonds formed between the nonpolar C_α proton of the Gly residue and the backbone carbonyl of the opposite helix (*39*). However, the individual affinities of all 18 single and/or double mutants were not readily rationalized by changes in van der Waals packing at the helix−helix interfaces or by changes in side-chain polarity. We therefore hypothesized that helix−lipid interactions might also contribute to the overall stability of the GpA and MCP dimers. If alteration of the lipid accessibility of the GpA and MCP monomers by small residue replacements in the $GG4_{GpA}$ and $GG4_{MCP}$ motifs influences stability as measured by the TOXCAT system, an inverse relationship between lipid solvation and dimer affinity should exist: more poorly solvated monomers would be expected to form stronger dimers and vice versa.

We therefore determined the total surface area of each WT and mutant GpA and MCP α-helix monomer accessible to a methylene-sized probe as an estimate of solvation by membrane components. This probe mimics the lipid acyl-chain radius in size, although it has considerably more conformational freedom than the covalently linked methylene groups in membrane lipids. In our analysis, a higher LASA represents more contact between lipid and protein (better solvation) and a lower LASA represents less contact (poorer solvation). Because the TM segments of both the NMR structure of GpA (*11*) and the MCP model (*17*) are α-helical, we generated energy-minimized α-helical structures (see the Experimental Procedures) that correspond to monomers of the WT and mutant GpA and MCP sequences placed in the TOXCAT construct (Figure 2) and analyzed the LASA of these helices. When the side-chain, backbone, nonpolar-group, and polar-group LASA values of the WT and mutant GpA and MCP helices were compared to their WT GpA-normalized TOXCAT signals (Figure 7), an inverse and statistically significant correlation between nonpolar LASA and dimer affinity was observed (R values of 0.75 for GpA, $p = 0.013$, and R values of 0.81 for MCP, $p = 0.004$; see Figure 7a). This correlation implies the existence of nonpolar cavities on the TM helix surface that have a role in determining affinity. Such cavities consist of local portions of nonpolar groups that cannot contact lipid and similar crevices that arise between adjacent nonpolar side chains. Note that cavities are distinct from the concave surfaces characteristic of GG4 motifs, which themselves are well-solvated by lipid. Helices with larger nonpolar LASAs form weaker dimers because a greater proportion of their nonpolar surface area can contact lipid and form favorable helix−lipid interactions. Those with smaller nonpolar LASAs have a greater proportion of their apolar surface excluded from lipid−helix interactions by steric constraints; viz., the methylene groups of lipid acyl chains cannot intercalate into these apolar cavities along the helix surface, precluding favorable interactions with membrane components and thereby driving these cavities to pair with a complementary surface.

In contrast, backbone and polar-group exposure to lipid was observed to only weakly correlate with dimer affinity (parts b and c of Figure 7). This relationship is easily rationalized, because the polar nature of peptide bonds and polar side chains precludes interaction with lipid: both seek a partner with which to form hydrogen bonds (*40*−*43*). The weak correlation coefficients observed for the backbone and polar-group parameters may also reflect the position specificity of hydrogen-bond formation, with the residues that are positioned correctly for interhelical hydrogen-bond formation contributing more to affinity, as is the case for the $SS4_{GpA}$ mutant (Figure 3). The inverse correlation observed for total side-chain LASA and affinity (Figure 7d) indicates that side-chain values are dominated by the nonpolar component, although correlations are weaker because of the inclusion of both polar and nonpolar groups in the side-chain calculation.

DISCUSSION

"Small-xxx-small" motifs are important contributory determinants to establishment of helix−helix interfaces in

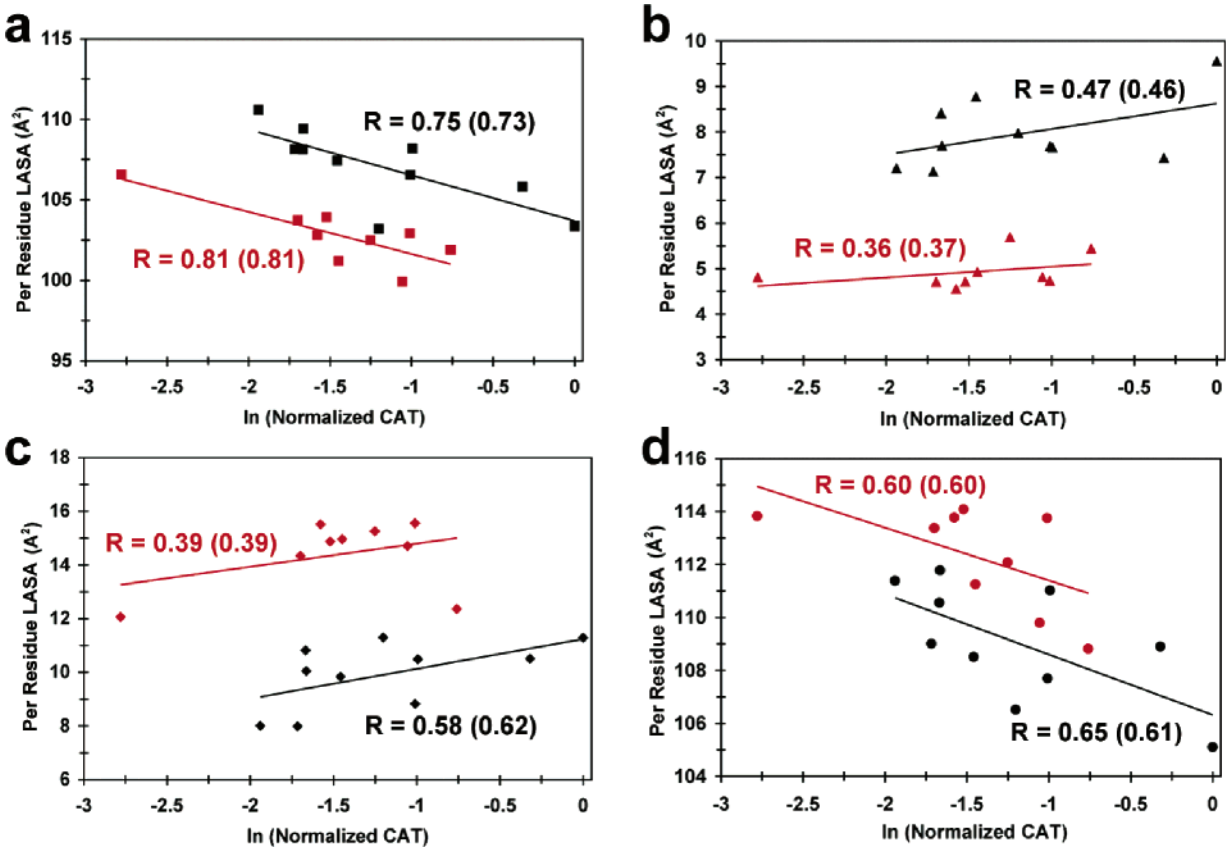

FIGURE 7: Relationship between dimer affinity and helix lipid accessibility. *Per residue* LASA of (a) nonpolar, (b) backbone, (c) polar, and (d) all side-chain atoms for WT and mutant GpA (black) and MCP (red) model helices, plotted versus the natural logarithm of the TOXCAT signal normalized to GpA WT. The *y*-axis scales of the graphs in a−d have been adjusted to allow for the display of both the GpA and MCP data sets. The G83I mutant of GpA is included in the data set, as are all of the GG4 motif mutants. The correlation coefficient of each linear fit determined by linear regression is indicated. Correlation coefficients given in parentheses indicate those calculated for each fit after measured [CAT] was normalized by densitometry values for Western band intensities. The correlations observed for per residue of nonpolar LASA and GpA or MCP affinity shown in a have $p = 0.013$ and 0.004, respectively.

membrane domains. However, because Gly residues are not specifically necessary for selection of the motif as the site of helix−helix contact, as evidenced by the preservation of the native interface in the $AS4_{MCP}$ double mutant V30L−F42T (Figure 5), there may be additional determinants of interface selection. Our finding that the presence of cavities on the TM helix surface inversely correlates with dimer affinity implies that the inability of lipid to solvate nonpolar surface area may also influence helix−helix interactions. Such cavities are unable to interact with lipid and could therefore be driven to find a complementary surface with which to pair. In the present work, we show that dimer affinity values in a library of 18 mutants in GpA and MCP dimers determined experimentally by the TOXCAT assay correlate with nonpolar-group lipid accessibility.

Measurement of TM−TM Dimer Affinity by the TOXCAT Assay. In establishing a correlation with LASA, it became of primary importance to determine accurate dimerization values. To this end, we quantitated expression by densitometry of the Western blots obtained from the full library of WT and mutant TOXCAT chimeras (Figure 3). Western blotting is the generally accepted control for chimera expression levels in the TOXCAT assay that has proven to be successful in measuring the effects of residue substitutions on helix affinity (*18*, *24*−*35*), even when compared to other methods for determining helix−helix affinity (*38*). We found that gel bands (Figure 3) had identical intensities ($p < 0.05$) with a range of ±13% for WT and mutant GpA and ±11% for WT and mutant MCP. When the measured intensities of each band were used to normalize the observed level of CAT expression, measured and densitometry-normalized CAT concentration values for each of the 18 WT and mutant constructs were found to be identical by *t* testing ($p < 0.01$). Further, we used the densitometry-normalized TOXCAT signals to recalculate our correlation coefficients (Figure 7). For both GpA and MCP, little or no change in the correlation coefficients was observed. Even those bands on the Western blot that visually appear to be darker, such as the GA4 mutant of GpA (Figure 3), actually report lower-than-WT CAT levels. In any case, the affinities of the WT and mutant GpA and MCP chimeras vary by up to 86% (for GpA) and 41% (for MCP). Therefore, it does not seem likely that variations in [CAT] resulting from chimera expression levels are biasing measurements of helix−helix association strength in our assays.

The in vivo TOXCAT measurements are made on helices embedded in the *E. coli* inner membrane, a lipid bilayer environment that itself is known to impose helicity on protein segments within it. However, one could consider the possibility that perturbation in *monomeric* helix structure and/or stability might be introduced by our residue substitutions in GpA and/or MCP. To address this point, we examined the total α-helix propensity in membrane-mimetic environments (*44*) for WT GpA, WT MCP, and all combinations

of Ala, Gly, and Ser replacements: for WT GpA and mutants, a mean per residue propensity of 3.05 ± 0.03 was calculated; for WT MCP and mutants, a mean per residue propensity of 3.38 ± 0.02 was calculated. The propensity to form α-helical structure thus varies by less than 1% among all of the WT and mutant GpA and MCP TM helix sequences tested in this work. Our CNS modeling of the individual helices that contain relatively conservative Gly-Ala-Ser replacements in terms of residue size and propensity for α-helix structure in apolar environments gives no suggestion of alteration in the WT GpA and/or MCP monomer structures. In this regard, it is interesting to note that GpA mutant G83I, in which Gly is mutated to the much higher helix-promoting residue Ile (*44*), actually loses more than 80% of its WT affinity, indicating that residue-dependent dimer affinity is most likely the dominant factor being measured in the TOXCAT assay.

Dimer Affinity Modulated by Gly, Ala, and Ser in Small-xxx-Small Motifs. Using Ala or Ser replacements to reduce the size of the concave GG4 interaction surface does not appear to influence the selection of this motif as the site of helix−helix contact in either the GpA or MCP homodimers, an observation consistent with MCP saturation mutagenesis experiments, where Ala and Ser were found to be the only residue substitutions in the motif that were compatible with its in vivo function (*45*). The identity of small residues in the GG4 motif (whether Gly, Ala, or Ser) is nevertheless capable of modulating affinity in context; this is the case in the GpA dimer, where Gly 79, the less buried of the two interfacial Gly residues, is more tolerant to residue substitution than its Gly 83 counterpart.

From this standpoint, one notes that the cavities found on the helix surfaces of *monomeric* GpA and MCP include residues that are found on the same helix face as the GG4 motif (Figure 8). Some of these residues surround the concave GG4 motif surface. For example, the lipid-occluded GpA residues Val 80 and Val 84 and MCP residue Ala 35 flank the GG4 motif and provide the "knobs" that pack into the Gly residue "holes" on their interaction partner. When a surface complementary to cavity-containing residues is provided into which they can intercalate, Gly residues may therefore contribute to but not completely specify helix−helix interaction sites, perhaps guiding the close approach of two helices, while unfavorable helix−lipid interactions at lipid-occluded residues provide an additional force for interface selection. The inability of lipid to solvate nonpolar cavities along the helix surface may therefore provide an additional force that drives the "knobs" into the Gly residue "holes".

If unfavorable helix−lipid interactions are the only determinants of interface selection, then the correlations between LASA and dimer affinity should be stronger when only interfacial residues are considered. However, we observe weaker correlations when only the interfacial GpA and MCP residues (*17*) are considered for all measures but polar groups (data not shown). This observation implies that lipid occlusion is a contributor but not the only criterion that specifies helix−helix interaction interfaces. In fact, residues that cannot be solvated by lipid, among them Ile 85 and Gly 86 in GpA and Lys 40 in MCP, remain lipid-exposed upon helix−helix interaction (Figure 8). A combination of forces must therefore influence which surfaces of two helices will

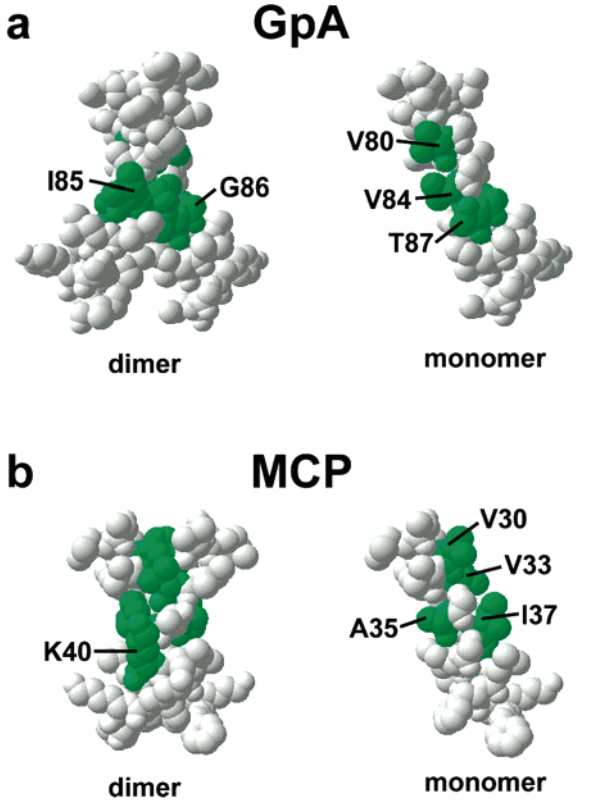

FIGURE 8: Lipid-inaccessible cavities on the GpA and MCP surfaces. Space-filling models of the TM helix regions of (a) the GpA homodimer (*11*) (PDB ID 1AFO) and (b) the MCP model (*17*) are shown. Dimeric structures are shown on the left; on the right, the topmost helix has been removed to reveal the interfacial residues. The five residues with the least accessible nonpolar surface area in the WT helices used for LASA calculations relative to an α-helical Gly-X-Gly reference peptide are shaded green. Residues labeled on the dimeric structures are lipid-inaccessible but non-interfacial; those labeled on the monomers are lipid-inaccessible and interfacial (compare with Figure 5). Note that many of the residues with lipid-inaccessible cavities surround the two Gly residues in the GG4 motif. This figure was produced with Swiss PDB Viewer (*54*).

pair with one another. Dimer stability most likely represents a balance between unfavorable helix−lipid and favorable helix−helix interactions, where unfavorable helix−lipid interactions might predominate in the forces that drive two helices into close proximity with one another, while favorable helix−helix interactions dictate the final interface selection and stability of each dimer (*40*, *41*). This balance is reflected by the observed minimum change of ∼5 Å^2 per residue in LASA for WT versus MCP mutants, which translates into ± ∼120 Å^2 per full-length helix, that correlates with TOXCAT-determined helix−helix interaction strength.

Lipid as a "Poor Solvent" for TM Helices. A possible role for lipid molecules in modulating the association of TM helices has been noted (for reviews, see refs *46* and *47*). For example, gains in conformational freedom by detergent molecules that are released during helix−helix association provide a small entropic contribution to the stability of the GpA dimer (*48*). Helix−helix interaction energy has also been shown to directly depend upon acyl-chain length (*49*), and mismatches between bilayer thickness and TM helix length are known to influence peptide oligomerization (*50*, *51*). Our observation that the affinity of the WT and mutant GpA and MCP homodimers is linked to poor lipid acces-

sibility of the entire helix surface contributes to the idea that unfavorable helix−lipid interactions may stabilize oligomers and perhaps help define their interaction site(s).

The roles of helix−helix and helix−lipid interactions in controlling and modulating the affinity of TM helix−helix associations have yet to be completely elucidated. Our results indicate that small (Ala and Ser) residue substitutions at the Gly positions in the GG4 motifs of GpA and MCP likely maintain the native helix−helix interface but alter affinity in a manner dependent upon the relative lipid exposure of nonpolar groups in the TM helix monomers. Although the exclusion of polar residues by lipid molecules likely dominates in helix−helix interactions, as evidenced by the formation of strong dimers by single polar residues (*41*, *52*) and burial of polar side chains according to a "lipophobic effect" (*53*), unfavorable helix−lipid interactions may also contribute to the stability of helix−helix association, particularly for those TM segments that form strong dimers in the absence of polar residues (*43*). In certain cases, lipid may therefore be considered as a less than ideal solvent for TM helices, conceptually analogous to water in soluble protein folding, and as such, can contribute to dimer stability and participate in defining helix−helix interfaces.

REFERENCES

1. White, S. H., and Wimley, W. C. (1999) Membrane protein folding and stability: Physical principles, *Annu. Rev. Biophys. Biomol. Struct. 28*, 319−365.
2. Opella, S. J., and Marassi, F. M. (2004) Structure determination of membrane proteins by NMR spectroscopy, *Chem. Rev. 104*, 3587−3606.
3. Rees, D. C., Chang, G., and Spencer, R. H. (2000) Crystallographic analyses of ion channels: Lessons and challenges, *J. Biol. Chem. 275*, 713−716.
4. Locher, K. P., Lee, A. T., and Rees, D. C. (2002) The *E. coli* BtuCD structure: A framework for ABC transporter architecture and mechanism, *Science 296*, 1091−1098.
5. Dutzler, R., Campbell, E. B., Cadene, M., Chait, B. T., and MacKinnon, R. (2002) X-ray structure of a CLC chloride channel at 3.0 Å reveals the molecular basis of anion selectivity, *Nature 415*, 287−294.
6. Jiang, Y., Lee, A., Chen, J., Cadene, M., Chait, B. T., and MacKinnon, R. (2002) Crystal structure and mechanism of a calcium-gated potassium channel, *Nature 417*, 515−522.
7. Jiang, Y., Lee, A., Chen, J., Ruta, V., Cadene, M., Chait, B. T., and MacKinnon, R. (2003) X-ray structure of a voltage-dependent K^+ channel, *Nature 423*, 33−41.
8. Popot, J. L., and Engelman, D. M. (2000) Helical membrane protein folding, stability, and evolution, *Annu. Rev. Biochem. 69*, 881−922.
9. Popot, J. L., and Engelman, D. M. (1990) Membrane protein folding and oligomerization: The two-stage model, *Biochemistry 29*, 4031−4037.
10. Engelman, D. M., Chen, Y., Chin, C. N., Curran, A. R., Dixon, A. M., Dupuy, A. D., Lee, A. S., Lehnert, U., Matthews, E. E., Reshetnyak, Y. K., Senes, A., and Popot, J. L. (2003) Membrane protein folding: Beyond the two stage model, *FEBS Lett. 555*, 122−125.
11. MacKenzie, K. R., Prestegard, J. H., and Engelman, D. M. (1997) A transmembrane helix dimer: Structure and implications, *Science 276*, 131−133.
12. Russ, W. P., and Engelman, D. M. (2000) The GxxxG motif: A framework for transmembrane helix−helix association, *J. Mol. Biol. 296*, 911−919.
13. Senes, A., Gerstein, M., and Engelman, D. M. (2000) Statistical analysis of amino acid patterns in transmembrane helices: The GxxxG motif occurs frequently and in association with β-branched residues at neighboring positions, *J. Mol. Biol. 296*, 921−936.
14. Schneider, D., and Engelman, D. M. (2004) Motifs of two small residues can assist but are not sufficient to mediate transmembrane helix interactions, *J. Mol. Biol. 343*, 799−804.
15. Doura, A. K., Kobus, F. J., Dubrovsky, L., Hibbard, E., and Fleming, K. G. (2004) Sequence context modulates the stability of a GxxxG-mediated transmembrane helix−helix dimer, *J. Mol. Biol. 341*, 991−998.
16. Doura, A. K., and Fleming, K. G. (2004) Complex interactions at the helix−helix interface stabilize the glycophorin A transmembrane dimer, *J. Mol. Biol. 343*, 1487−1497.
17. Melnyk, R. A., Kim, S., Curran, A. R., Engelman, D. M., Bowie, J. U., and Deber, C. M. (2004) The affinity of GxxxG motifs in transmembrane helix−helix interactions is modulated by long-range communication, *J. Biol. Chem. 279*, 16591−16597.
18. Russ, W. P., and Engelman, D. M. (1999) TOXCAT: A measure of transmembrane helix association in a biological membrane, *Proc. Natl. Acad. Sci. U.S.A. 96*, 863−868.
19. Li, R., Gorelik, R., Nanda, V., Law, P. B., Lear, J. D., DeGrado, W. F., and Bennett, J. S. (2004) Dimerization of the transmembrane domain of integrin αIIb subunit in cell membranes, *J. Biol. Chem. 279*, 26666−26673.
20. Hubbard, S. J., and Thornton, J. M. (1993) "NACCESS", Computer Program, Department of Biochemistry and Molecular Biology, University College London, U.K.
21. Shrake, A., and Rupley, J. A. (1973) Environment and exposure to solvent of protein atoms. Lysozyme and insulin, *J. Mol. Biol. 79*, 351−371.
22. Chothia, C. (1975) Structural invariants in protein folding, *Nature 254*, 304−308.
23. Brunger, A. T., Adams, P. D., Clore, G. M., DeLano, W. L., Gros, P., Grosse-Kunstleve, R. W., Jiang, J. S., Kuszewski, J., Nilges, M., Pannu, N. S., Read, R. J., Rice, L. M., Simonson, T., and Warren, G. L. (1998) Crystallography and NMR system: A new software suite for macromolecular structure determination, *Acta Crystallogr., Sect. D: Biol. Crystallogr. 54* (part 5), 905−921.
24. Russ, W. P., and Engelman, D. M. (2000) The GxxxG motif: A framework for transmembrane helix−helix association, *J. Mol. Biol. 296*, 911−919.
25. Mendrola, J. M., Berger, M. B., King, M. C., and Lemmon, M. A. (2002) The single transmembrane domains of ErbB receptors self-associate in cell membranes, *J. Biol. Chem. 277*, 4704−4712.
26. Melnyk, R. A., Kim, S., Curran, A. R., Engelman, D. M., Bowie, J. U., and Deber, C. M. (2004) The affinity of GXXXG motifs in transmembrane helix−helix interactions is modulated by long-range communication, *J. Biol. Chem. 279*, 16591−16597.
27. McClain, M. S., Iwamoto, H., Cao, P., Vinion-Dubiel, A. D., Li, Y., Szabo, G., Shao, Z., and Cover, T. L. (2003) Essential role of a GXXXG motif for membrane channel formation by *Helicobacter pylori* vacuolating toxin, *J. Biol. Chem. 278*, 12101−12108.
28. McClain, M. S., Cao, P., and Cover, T. L. (2001) Amino-terminal hydrophobic region of *Helicobacter pylori* vacuolating cytotoxin (VacA) mediates transmembrane protein dimerization, *Infect. Immun. 69*, 1181−1184.
29. Li, R., Gorelik, R., Nanda, V., Law, P. B., Lear, J. D., DeGrado, W. F., and Bennett, J. S. (2004) Dimerization of the transmembrane domain of Integrin αIIb subunit in cell membranes, *J. Biol. Chem. 279*, 26666−26673.
30. Li, R., Bennett, J. S., and Degrado, W. F. (2004) Structural basis for integrin αIIbβ3 clustering, *Biochem. Soc. Trans. 32*, 412−415.
31. Johnson, R. M., Heslop, C. L., and Deber, C. M. (2004) Hydrophobic helical hairpins: Design and packing interactions in membrane environments, *Biochemistry 43*, 14361−14369.
32. Dawson, J. P., Melnyk, R. A., Deber, C. M., and Engelman, D. M. (2003) Sequence context strongly modulates association of polar residues in transmembrane helices, *J. Mol. Biol. 331*, 255−262.
33. Dawson, J. P., Weinger, J. S., and Engelman, D. M. (2002) Motifs of serine and threonine can drive association of transmembrane helices, *J. Mol. Biol. 316*, 799−805.
34. Constantinescu, S. N., Keren, T., Russ, W. P., Ubarretxena-Belandia, I., Malka, Y., Kubatzky, K. F., Engelman, D. M., Lodish, H. F., and Henis, Y. I. (2003) The erythropoietin receptor transmembrane domain mediates complex formation with viral anemic and polycythemic gp55 proteins, *J. Biol. Chem. 278*, 43755−43763.
35. Chin, C. N., Sachs, J. N., and Engelman, D. M. (2005) Transmembrane homodimerization of receptor-like protein tyrosine phosphatases, *FEBS Lett. 579*, 3855−3858.

36. Sulistijo, E. S., Jaszewski, T. M., and MacKenzie, K. R. (2003) Sequence-specific dimerization of the transmembrane domain of the "BH3-only" protein BNIP3 in membranes and detergent, *J. Biol. Chem. 278*, 51950−51956.
37. Dawson, L. P., Melnyk, R. A., Deber, C. M., and Engelman, D. M. (2003) Sequence context strongly modulates association of polar residues in transmembrane helices, *J. Mol. Biol. 331*, 255−262.
38. Fleming, K. G., and Engelman, D. M. (2001) Specificity in transmembrane helix−helix interactions can define a hierarchy of stability for sequence variants, *Proc. Natl. Acad. Sci. U.S.A. 98*, 14240−14244.
39. Senes, A., Ubarretxena-Belandia, I., and Engelman, D. M. (2001) The Ca−H···O hydrogen bond: A determinant of stability and specificity in transmembrane helix interactions, *Proc. Natl. Acad. Sci. U.S.A. 98*, 906−9061.
40. Zhou, F. X., Cocco, M. J., Russ, W. P., Brunger, A. T., and Engelman, D. M. (2000) Interhelical hydrogen bonding drives strong interactions in membrane proteins, *Nat. Struct. Biol. 7*, 154−160.
41. Gratkowski, H., Lear, J. D., and DeGrado, W. F. (2001) Polar side chains drive the association of model transmembrane peptides, *Proc. Natl. Acad. Sci. U.S.A. 98*, 880−885.
42. Choi, M. Y., Cardarelli, L., Therien, A. G., and Deber, C. M. (2004) Non-native interhelical hydrogen bonds in the cystic fibrosis transmembrane conductance regulator domain modulated by polar mutations, *Biochemistry 43*, 8077−8083.
43. Johnson, R. M., Heslop, C. L., and Deber, C. M. (2004) Hydrophobic helical hairpins: Design and packing interactions in membrane environments, *Biochemistry 43*, 14361−14369.
44. Liu, L. P., and Deber, C. M. (1998) Uncoupling hydrophobicity and helicity in transmembrane segments. α-Helical propensities of the amino acids in non-polar environments, *J. Biol. Chem. 273*, 23645−23648.
45. Williams, K. A., Glibowicka, M., Li, Z., Li, H., Khan, A. R., Chen, Y. M. Y., Wang, J., Marvin, D. A., and Deber, C. M. (1995) Packing of coat protein amphipathic and transmembrane helices from filamentous bacteriophage M13: Role of small residues in protein oligomerization, *J. Mol. Biol. 252*, 6−14.
46. Lee, A. G. (2003) Lipid−protein interactions in biological membranes: A structural perspective, *Biochim. Biophys. Acta 1612*, 1−40.
47. Lee, A. G. (2004) How lipids affect the activities of integral membrane proteins, *Biochim. Biophys. Acta 1666*, 62−87.
48. Fisher, L. E., Engelman, D. M., and Sturgis, J. N. (1999) Detergents modulate dimerization, but not helicity, of the glycophorin A transmembrane domain, *J. Mol. Biol. 293*, 639−651.
49. Mall, S., Broadbridge, R., Sharma, R. P., East, J. M., and Lee, A. G. (2001) Self-association of model transmembrane α-helices is modulated by lipid structure, *Biochemistry 40*, 12379−12386.
50. Cristian, L., Lear, J. D., and DeGrado, W. F. (2003) Use of thiol-disulfide equilibria to measure the energetics of assembly of transmembrane helices in phospholipid bilayers, *Proc. Natl. Acad. Sci. U.S.A. 100*, 14772−14777.
51. Killian, J. A. (2003) Synthetic peptides as models for intrinsic membrane proteins, *FEBS Lett. 555*, 134−138.
52. Zhou, F. X., Merianos, H. J., Brunger, A. T., and Engelman, D. M. (2001) Polar residues drive association of polyleucine transmembrane helices, *Proc. Natl. Acad. Sci. U.S.A. 98*, 2250−2255.
53. Adamian, L., Nanda, V., DeGrado, W. F., and Liang, J. (2005) Empirical lipid propensities of amino acid residues in multispan α helical membrane proteins, *Proteins 59*, 496−509.
54. Guex, N., and Peitsch, M. C. (1997) SWISS-MODEL and the Swiss-PdbViewer: An environment for comparative protein modeling, *Electrophoresis 18*, 2714−2723.

BI060063F